HHS Public Access

Author manuscript

J Biomed Mater Res A. Author manuscript; available in PMC 2023 February 16.

Published in final edited form as:

J Biomed Mater Res A. 2017 January ; 105(1): 159–168. doi:10.1002/jbm.a.35896.

Design and demonstration of an intracortical probe technology with tunable modulus

Dustin M. Simon[1], **Hamid Charkhkar**[2], **Conan St. John**[3], **Sakthi Rajendran**[3], **Tong Kang**[3], **Radu Reit**[3], **David Arreaga-Salas**[3], **Daniel G. McHail**[4], **Gretchen L. Knaack**[4], **Andrew Sloan**[3], **Dane Grasse**[3], **Theodore C. Dumas**[4], **Robert L. Rennaker**[3], **Joseph J. Pancrazio**[3,5], **Walter E. Voit**[1,3]

[1]Department of Materials Science and Engineering, The University of Texas at Dallas, Richardson, Texas 75030

[2]Department of Electrical and Computer Engineering, George Mason University, Fairfax, Virginia 22030

[3]Department of Bioengineering, The University of Texas at Dallas, Richardson, Texas 75030

[4]Department of Molecular Neuroscience, The Krasnow Institute for Advanced Study, George Mason University, Fairfax, Virginia 22030

[5]Department of Bioengineering, George Mason University, Fairfax, Virginia 22030

Abstract

Intracortical probe technology, consisting of arrays of microelectrodes, offers a means of recording the bioelectrical activity from neural tissue. A major limitation of existing intracortical probe technology pertains to limited lifetime of 6 months to a year of recording after implantation. A major contributor to device failure is widely believed to be the interfacial mechanical mismatch of conventional stiff intracortical devices and the surrounding brain tissue. We describe the design, development, and demonstration of a novel functional intracortical probe technology that has a tunable Young's modulus from ~2 GPa to ~50 MPa. This technology leverages advances in dynamically softening materials, specifically thiol-ene/acrylate thermoset polymers, which exhibit minimal swelling of < 3% weight upon softening *in vitro*. We demonstrate that a shape memory polymer-based multichannel intracortical probe can be fabricated, that the mechanical properties are stable for at least 2 months and that the device is capable of single unit recordings for durations up to 77 days *in vivo*. This novel technology, which is amenable to processes suitable for manufacturing via standard semiconductor fabrication techniques, offers the capability of softening *in vivo* to reduce the tissue-device modulus mismatch to ultimately improve long term viability of neural recordings.

Keywords

brain machine interface; intracortical microelectrode array; neural interface; shape memory polymer; neural recording

Correspondence to: W. E. Voit; walter.voit@utdallas.edu.

INTRODUCTION

Neuroscientists rely on arrays of microelectrodes to probe the functional circuitry of the brain underlying neural function and behavior.[1,2] Clinically, microscale intracortical probes offer the promise of bypassing damaged regions of the nervous system to reduce the burden of paralysis and limb loss.[3,4] A major limitation of existing intracortical probe technology pertains to limited lifetime of recording after implantation with current implantation limits of approximately two years before devices fail.[5,6] One of the causes for this failure is believed to originate from the chronic foreign body response by microglia and astrocytes which occurs 2 and 4 weeks following implantation that was not observed in microelectrode stab wound controls.[7,8] This foreign body response has often been attributed in large part to the mechanical mismatch that exists between the materials that comprise intracortical probes and the surrounding brain tissue.[8–10] State-of-the-art intracortical probes are primarily made from high modulus materials such as tungsten and silicon which have an elastic modulus that is six orders of magnitude greater than brain tissue. Several groups have suggested that motion of the brain with respect to the probe may induce damage to the surrounding tissue and exacerbate the foreign body response.[9–14] Specifically, probes consisting of high modulus materials induce strain and trigger inflammation in the surrounding brain tissue. This article describes the design, development and demonstration of a novel functional intracortical probe technology that has a tunable modulus. This technology leverages advances in dynamically softening materials, specifically thiol-ene/acrylate thermoset polymers, which soften due to fluid uptake and temperature change in the minutes to hours following implantation. The goal of this work was to show that: (1) a multichannel intracortical probe can be fabricated using shape memory polymers (SMPs) consisting of thiol-ene/acrylate thermoset polymers, (2) devices can be fabricated from polymer formulations that allow tunable dynamic mechanical properties, and (3) a functional intracortical probe fabricated using SMPs exhibits *in vitro* biocompatibility and *in vivo* neural recordings consistent with the performance of conventional implantable devices. Dynamic mechanical analysis and differential scanning calorimetry were used to evaluate the thermomechanical properties of SMPs whereas *in vivo* electrophysiology and immunohistochemistry were applied to a prototype SMP intracortical probe to show proof-of-concept functionality. We demonstrate that a SMP-based multichannel intracortical probe can be fabricated and the electrical behavior *in vitro* and *in vivo* is consistent with the performance of conventional implantable devices. This technology, based on advances in thin film flexible electronics processing, offers the capability of softening *in vivo* to reduce the tissue-device modulus mismatch.

METHODS

Polymer synthesis

Tricyclo[5.2.1.$0^{2,6}$]decanedimethanol diacrylate (TCMDA), 1,3,5-triallyl-1,3,5-triazine-2,4,6(1H,3H,5H)-trione (TATATO), tris[2-(3-mercaptopropionyloxy)ethyl] isocyanurate (TMICN), 2,2-dimethoxy-2-phenyl acetophenone (DMPA), phosphate buffered saline (PBS), poly(vinyl alcohol), ethylenedioxythiophene (EDOT), and poly(sodium 4-styrenesultanate)(PSS) were purchased from Sigma Aldrich.

Detailed synthesis of the SMP substrates has been previously reported.[15] To explore the feasibility of our approach, we fabricated material samples with TCMDA concentrations of 31% and 47%. The thiol-ene/acrylate (31% TCMDA) substrate was prepared by mixing a solution of a stoichiometric ratio of TATATO and TMICN to which was added 31 mol % TCMDA and 0.1 wt % DMPA as a photoinitiator. The thiol-ene/acrylate (47% TCMDA) substrate was prepared by mixing a solution of a stoichiometric ratio of TATATO and TMICN to which was added 47 mol % TCMDA and 0.1 wt % DMPA as a photoinitiator. Both monomer solutions were placed in a parallel plate glass mold with a thickness of 0.035 mm or 1 mm and polymerized in a crosslinking chamber with 365 nm UV light (Cole Parmer, UVP CL-1000 Ultraviolet Crosslinker).

Thermomechanical analysis

Dynamic mechanical analysis (DMA) and differential scanning calorimetry (DSC) were used to characterize the thermomechanical properties of the polymer formulations. DMA was performed using a Mettler Toledo DMA 861e/SDTA in a manner previously described.[15] Samples were cut into cylinders approximately 1 mm thick and 3 mm in diameter. The shear deformation mode covered approximately 70% of the surface area of the sample which was in contact with the clamping assembly which limited water evaporation. DMA was performed twice for each composition where T_g was denoted as the peak of tan δ. Dry samples were tested from 0 to 100°C. In addition, DSC was performed on a Mettler Toledo DSC 1 with an intracooler option in a manner previously described.[14] Dry samples were heated from room temperature to 100°C, cooled to −50°C, and heated to 200°C. Data shown are of only the second heating cycle. The heating and cooling rate was fixed at 10°C/min. Swollen samples were cooled immediately to −50°C and then heated to 100°C. Data were only collected for the one cycle to limit effects of moisture desorption during heating. Tests were conducted in a nitrogen atmosphere. For DSC, T_g was denoted as the midpoint of the thermal transition.

Characterization of polymer swelling

Polymer samples were cut into approximately 15 mg pieces of 0.125 mm thickness such that swollen sample weight could be measured six times at each time point of 1, 7, and 28 days. Samples were placed in sealed glass vials containing phosphate buffered saline (PBS) and placed in an oven at 37°C. Moisture absorption of the thiol-ene/acrylate composition was measured by change in weight over time in the simulated physiological conditions (37°C, PBS). Swelling percent, q, was determined according to the formula:

$$q(\%) = \frac{w_s - w_i}{w_i} \times 100 \quad (1)$$

where w_s was the swollen weight and w_i was the initial, dry sample weight.

Accelerated aging

To estimate the long-term change in mechanical properties, polymer samples of each material were placed in vials filled with PBS. The vials were then sealed and placed in

an oven at 90°C. For accelerated aging experiments, the simulated time (T_{sim}) is related to the actual experiment time (T_{exp}) as follows:

$$T_{sim} = T_{exp} \cdot Q_{10}^{\Delta T/10} \quad (2)$$

where $\Delta T = T - 37$°C, T is the elevated temperature at which aging takes place, and Q_{10} is the temperature coefficient which is assumed to be two.[16] Samples for 31% and 47% TCMDA were soaked for 4, 26, and 48 h at 90°C to accelerate aging by a factor of 40 such that time intervals correspond to 1, 6, and 11 weeks under physiological conditions. Accelerated aging samples (pre-cut to 1 mm thick, 3 mm diameter) were removed from the sample vial and tested in shear parallel-plate configuration via DMA between 25 to 50°C as described above.

Device fabrication

The thin film layers, 300 nm of e-beam evaporated Au and 1 μm of chemical-vapor-deposited parylene-C, were patterned using standard photolithography processes in a Class 10,000 cleanroom located at the University of Texas at Dallas. A solution consisting of 1% poly(vinyl alcohol) (PVA) in deionized water was placed on top of fabricated devices and allowed to dry over night at room temperature to use as a sacrificial protective layer to protect the device from organics being redeposited onto electrodes during laser micromachining.

The final device geometry [a single multielectrode device similar to a Neuronexus architecture, shown in Figure 4(A–C)] was formed using laser micromachining with a Spectra-Physics HIPPO (λ = 355 nm) Q-switched laser and μFab station. The average laser power as 2.5 mW/cm^2. The repetition rate was 100 kHz. The beam diameter averaged 7 mm, but ranged from 4–10 mm. The pulse duration averaged 12 ns, but ranged from 7–16 ns. Thus the radiant fluence was approx. 2.5 ×10^{-5} mJ/cm^2.

The sacrificial PVA layer was finally removed through a hard mask using O_2 plasma etching in a Technics RIE for 3 min with 200 mtorr of O_2 and 200 W of power and a 5 min rinse in deionized water, a cleaning step that removed any excess or trapped PVA, not etched away.

To lower the electrochemical impedance, the 177 μm^2 circular microelectrode contacts [Fig. 4(A)] were coated with poly(3,4-ethylenedioxythiophene) polystyrene sulfonate (PEDOT:PSS). A solution of 10 mM EDOT in 0.1 mM PSS sodium salt in deionized water was prepared and PEDOT:PSS was deposited under galvanostatic conditions with 1.2 C/cm^2 or 0.64 μC for each microelectrode such that the charge injection for the PEDOT:PSS deposition was consistent with prior work.[17] Electrochemical impedance spectroscopy (EIS) (Model 600 Series, CH Instruments, Austin, TX) was performed before and after the deposition to confirm the reduction in the impedance of the microelectrodes. The frequency range for the EIS was set from 0.1 Hz to 100 kHz, a 20 mV_{p-p} sinusoid signal was used as input, and the reference and counter electrodes were Ag/AgCl and Pt, respectively.

For scanning electron microscopy (SEM) imaging, a thin layer of Au/Pd alloy was sputtered onto the devices to avoid accumulation of a negative charge on the surface of the device.

In vitro functional neurotoxicity

To assess the functional neurotoxicity of the substrate materials, we utilized the procedure described by Charkhkar and colleagues.[18] Rectangular samples of the two polymer formulations were fabricated with the dimensions of 8 mm long, 10 mm wide, and 0.5 mm thickness. Frontal cortex tissue was isolated and extracted from embryonic day 17 mice.[18,19] The tissue was dissociated and then seeded on commercially-available microelectrode arrays (MEAs; Multi Channel Systems, Reutlingen, Germany) where substrates had been coated with poly-d-lysine (Sigma-Aldrich, St Louis, MO) and laminin (Sigma-Aldrich). The cultures were maintained in an incubator (37°C and 10% CO_2) and were provided with DMEM–based media twice a week. Between days 21–28 *in vitro*, when the cultures formed mature networks, the baseline spontaneous activity was recorded for 15 min. The *in vitro* extracellular recordings were performed using a 64-channel OmniPlex neural data acquisition system (Plexon, Dallas, TX). The neuronal networks were then incubated for 24 h with the extracts of the sample polymers. After the incubation time, a postexposure recording was performed. The reduction in the spiking activity compared to the baseline was considered as a measure of functional toxicity.[18]

Surgery and probe implantation

The goal of the *in vivo* work was to demonstrate feasibility of a prototype SMP-based intracortical probe capable of recording neural activity for at least 2 months, a period of time which is twice as long as a comparative study examining intracortical probe stability profiles.[20] NIH guidelines for the care and use of laboratory animals (NIH Publication #85–23 Rev. 1985) have been observed. All animal procedures in this work were approved by the Institutional Animal Care and Use Committee at George Mason University, Fairfax, VA. Two adult female Long Evans rats weighing 250–350 g were anesthetized with 5% isoflurane oxygen mixture at a rate of 1 L/min and maintained with 1% after an intraperitoneal injection of xylazine (AgriLabs, St. Joseph, MO) at 13.33 mg/kg. Dexamethasone (AgriLabs), as a precaution against tissue swelling, at 2 mg/kg and 0.5% lido-caine (AgriLabs) were injected subcutaneously under the targeted incision site. The skull was exposed and cleaned with three alternations of 70% ethanol and 3% hydrogen peroxide, finishing with ethanol. Avoiding blood vessels, six skull screws were placed in burr holes drilled with a micro drill. After locating bregma, the craniotomy window of 12 mm^2 was prepared at −2.0 to +2.0 mm anterior/posterior and 0.5 to 2.5 mm medial/lateral. The stainless steel ground and reference wires, 3 cm long with 2 cm deinsulted from the tip of the wires, were secured to separate skull screws and coated with conductive silver paint to ensure electrical continuity. A hole was made in dura just below the tip of the probe and then the probe was lowered to the surface of the cortex. To constrict local blood vessels, gauze moistened with epinephrine at 1:1000 by volume within 0.9% saline was applied. The probe was inserted using a micropositioner and advanced by 100 μm increments every 40 s to a final depth of 1700–2000 μm. Neuronal spiking was monitored throughout insertion and a position was located where activity could be recorded on at least half of the microelectrode sites. The craniotomies were filled with silicone elastomer (Kwik-Cast, World Precision Instruments, Sarasota, FL). A layer of Loctite Prism 454 adhesive (Electron Microscopy Science, Hatfield, PA) was also applied and cured instantly with Loctite accelerant 7452 (Newark Element 14, Chicago, IL) to secure the device to the skull and

screws. Dental cement (Lang Dental Manufactures, Wheeling, IL) was used to additionally secure the screws to the skull and create a robust head cap. To reduce post-surgical pain and inflammation, ketoprofen (Vet Depot, Encinitas, CA) was administered subcutaneously at 5 mg/kg and continued twice daily for three days. To reduce the likelihood of bacterial infection, gentamicin (SouthernBiotech, Birmingham, AL) was also injected subcutaneously at 8 mg/kg and continued once a day for 1 week.

Neural recordings and analysis

Neural signals were recorded in rats two days after surgery followed by weekly recordings for over two months. Each recording session lasted for 10 min. Data were acquired using a Cerebus system (Blackrock Microsystems, Salt Lake City, UT) and each channel was recorded at 30,000 samples per second. To remove any movement artifacts associated with recording from awake animals, a common average reference was subtracted from each channel[21] using a custom-routine in MATLAB (Mathworks, Natick, MA). Spikes were detected by signal magnitude excursions of beyond a threshold. Each channel had a specific threshold based on six standard deviations of the baseline noise for that channel. The captured spikes were then sorted for each channel into well-resolved units in Offline Sorter V.3 (Plexon, Inc, Dallas, TX) and confirmed by visual inspections. Peak-to-peak amplitude ($V_{p\text{-}p}$) and spike rate were calculated for each unit. The signal-to-noise ratio (SNR) for each unit was defined as the mean $V_{p\text{-}p}$ over root mean square (RMS) value of the noise for the corresponding unit.

In vivo impedance measurement

Consistent with neural recording, impedance measurements were also performed two days and then weekly after the probe implantation. To reduce noise in data collection due to motion artifacts, the animals were anesthetized with 1 L/min oxygen and 5% isoflurane. Impedance was measured using a CH instrument electrochemical analyzer (CH Instruments) at 1 kHz with an input signal of 20 mV.

Device capture immunohistochemistry

Rats were sacrificed by exsanguination from transcardial perfusion after anesthetizing with a 5% isoflurane/oxygen mixture (1 L/min) until no pain response was observed. Blood was cleared with phosphate buffered saline (1× PBS, Fisher Scientific, Pittsburg, PA) followed by 4% paraformaldehyde (PFA) to fix the tissue. The entire head was placed in PFA for 48 h and then stored in PBS containing 90 mg/L sodium azide (Sigma-Aldrich, St. Louis, MO) at 4°C until head caps were removed (all subsequent steps with PBS contain sodium azide). Head caps were removed with the probes remaining in the brain for device capture immunohistochemistry (IHC).[22] Briefly, dental cement and adhesive were removed by first cutting with a Dremel cutting wheel followed by drilling with a micro drill bit. The probes were separated at the base from the silicone elastomer using microscissors. The elastomer was then removed using for-ceps and the skull was carefully detached from the brain leaving the probes intact. All of these steps were performed under a surgical scope. Brains containing the probes were then placed in fresh PBS with sodium azide and stored at 4°C until slicing.

Brains were sliced in the sagittal plane (200–250 μm) with a vibratome, such that one slice contained the entire probe. Free-floating sections were placed in a single well of a 24-well culture plate containing PBS. All slices were labeled with primary antibodies for neurons (chicken anti-NeuN, Millipore, Billerica, MA), reactive microglia/macro-phages (monoclonal mouse anti-ED1 CD68, Millipore, Billerica, MA), glial fibrillary acidic protein of activated astrocytes (rabbit anti-GFAP, Dako North America Inc., Carpinteria, CA), and cellular nuclei (DAPI, Life Technologies, Grand Island, NY).

Auto fluorescence was quenched two times with 6 mg/mL sodium borohydrate (Sigma-Aldrich) for 15 min each, followed by three washes with PBS for 5 min each. Sections were incubated in blocking buffer containing 4% normal goat serum (Life Technologies) and 0.3% Triton-X 100 (Sigma-Aldrich) in PBS for 1 h followed by three rapid washes with PBS. Slices were additionally blocked with Image-iT FX (Life Technologies) for 30 min followed by three rapid washes in PBS. Slices were then incubated over-night at 4°C in primary antibody solution (CD68 1:1000, GFAP 1:500, NeuN 1:500 diluted in blocking buffer containing 4% normal goat serum and 0.1% Triton-X 100 in PBS). Following four washes with PBS for 15 min each, slices were incubated for 1 h at room temperature in fluorophore-conjugated secondary antibodies (goat anti-chicken 647, goat anti-mouse 546, goat anti-rabbit 488, 1:1000, Life Technologies), and DAPI (0.6 μM) diluted in the same blocking buffer used for the primary antibodies. To ensure homogenous penetration of all solutions slices were flipped half way through each step. Lastly, slices were washed three times in PBS for 15 min each and mounted on glass microscope slides using Fluoromount-G (Southern Biotech, Birmingham, AL).

RESULTS

Polymer composition and thermomechanical properties

SMP substrates were fabricated on a thiol-ene/acrylate polymer substrate comprised of TATATO and TMICN with TCMDA and photoinitiator. The substrates were formed by a stoichiometric ratio of TATATO and TMICN with 31 or 47 mol % TCMDA to create a thermosetting network. The basis of the polymer network are the ene-functional and thiol-functional monomers, TATATO and TMICN, respectively, which provide a low cure stress film and good adhesion to Au films to support the microfabrication process. Figure 1(a) shows the shear storage modulus, G', of the two compositions in the dry state measured by DMA as a function of temperature. Each composition exhibited an onset of T_g above 37°C such that an intracortical device fabricated from these polymer formulations would be sufficiently stiff to penetrate brain tissue. By changing the ratio of TCMDA, a rigid diacrylate monomer, to other monomers in the composition the polymer network can be modified to have a higher rubbery modulus and higher T_g with increasing amount TCMDA, because the resulting more sterically hindered polymer network makes softening occur at a higher temperature. For example, the rubbery modulus increased slightly from 3.86 ± 0.07 MPa to 3.97 ± 0.18 MPa for 31 and 47 mol % TCMDA. The T_g, defined as the peak of tan δ in Figure 1(b), of the 31 mol % composition was 58°C and increased to 67°C for 47 mol % TCMDA. While TATATO and TMICN can only homopolymerize, the TCMDA monomer can polymerize with both thiol or acrylate functional groups to generate a more

heterogeneous network, an observation consistent with the lower and broader tan δ curve for 47 mol % TCMDA. These two compositions provide processing stability to fabricate virtually identical intracortical probes, but subtle changes in network properties will allow tunable mechanical characteristics when implanted in tissue. For comparison, cortical tissue typically has a Young's modulus below 40 kPa such that devices can be inserted with a shear modulus near ~600 MPa (Young's modulus ~1.8 GPA) and soften toward the modulus of the tissue. The degree of softening *in vivo* depends upon many factors, but we predict softening *in vivo* to below ~30 MPa in shear modulus, approaching the modulus of tissue, but still orders of magnitude stiffer than the surrounding tissue.

Thermomechanical properties *in vitro*

In Figure 2(a), the moisture absorption of each polymer composition is shown after exposure to PBS at 37°C. After 28 days, the polymers absorbed 2.96 ± 0.07% and 2.44 ± 0.23% water for 31 and 47 mol % TCMDA, respectively, indicative of a low degree of swelling *in vitro*. The polymers will continue to swell, but appear to be tapering off in water uptake. The 28 day time point *in vitro* provides a reasonable swelling estimate for month-long sub-chronic studies. DSC was used to measure the change in T_g, via analysis of heat flow during thermal cycling, for the polymer formulations due to plasticization [Fig. 2(b)] of water into the polymer network. Plasticization, due to fluid uptake, causes a disentangling of the polymer network and increases molecular motion resulting in a decrease in the T_g. The 31 mol % TCMDA composition showed a larger shift to a lower T_g compared to the 47 mol % TCMDA composition. This difference may be due to the TCMDA monomer adding a more hydrophobic backbone to the network than the other monomers and effectively contributing a larger proportion of the overall polymer network. The endothermic peaks near 0°C for the 31 mol % formulation can be attributed to the presence of free water within the polymer network that is not tightly bound to the polymer chains. The effect of moisture absorption and decrease in T_g appears to result in an isothermal decrease in modulus at 37°C for both polymer compositions as shown in Figure 2(c). Samples were exposed to accelerated aging conditions to examine the changes in mechanical properties over time. The change in shear storage modulus, G′, closely follows the change in swelling content *in vitro*. After 48 h at 90°C, which simulates 77 days under physiological conditions, the modulus at 37°C decreased from approximately 600 MPa to 27.5 ± 8.9 MPa and 140.4 ± 20.2 MPa for 31 and 47 mol % TCMDA, respectively. This difference in modulus between the two compositions is driven by (1) the initial T_g of each polymer and (2) the extent of plasticization due to moisture absorption. This difference in modulus coupled with low levels of moisture absorption are key material properties that make these polymer formulations useful in the development of a novel class of softening intracortical probes.

In vitro functional neurotoxicity

In vitro cytotoxicity testing is a useful step in assessing the putative biocompatibility of novel implantable materials as described by the international standard ISO 10993. Recent guidance released in 2013 by ASTM International F2901 concerning the tests for potential neurotoxicity of medical devices recognizes limitations in non-neural derived cells for *in vitro* testing. Consistent with Harry et al.[23] F2901 recommends the use of cells derived from nervous tissue to provide a more comprehensive assessment. We utilized a recently

developed method to quantify the effect of materials on bioelectrical activity from cultured neuronal networks as a functional assay for neurotoxicity. As shown in Figure 3, the polymer samples were tested on the neuronal cultures *in vitro* to assess the functional toxicity of the material prior to implantation. In total, eight neuronal networks were utilized in the tests, four for each material. Neuronal cultures had the baseline spike rate of 6.4 ± 2.2 Hz and 60.8 ± 18.1% of the electrodes showed spontaneous activity. The normalized spike rate after 24 h of extract exposure for 47 mol % TCMDA was 0.96 ± 0.14 and for 31 mol % TCMDA was 0.94 ± 0.1 (N = 4 networks for each formulation) suggesting no significant neurotoxicity effects of the tested materials. Compared to conventional cytotoxicity methods such as live/dead assays, it was shown that the functional toxicity method based on neuronal cultures on MEAs could provide endpoints that are more relavant to brain-computer interface applications.[18] This result demonstrates that controlled changes in polymer chemistry can be implemented which produce materials with little or no *in vitro* neurotoxicity.

Fabrication of polymer intracortical probes and modification with PEDOT:PSS

The polymer chemistry chosen for this work was specifically designed such that the probe is stiff during implantation and can soften postimplantation. To demonstrate that a functional intracortical probe can be fabricated with our approach, we focused on a single polymer formulation using 47 mol % TCMDA. Figure 4(a–c) show the features of the intracortical probe at the scale of an individual microelectrode site, penetrating probe, and the interface board for coupling with the recording system. The probe and microelectrode geometry was chosen to be comparable to dimensions associated with commercially available devices. The diameter of each microelectrode is 15 μm, which corresponds to a geometric surface area of 177 μm^2. To reduce the impedance of the Au microelectrodes, each was modified with PEDOT:PSS [Fig. 4(a)]. The penetrating portion of the probe was designed with a 2.5 mm long tip with electrodes evenly spaced linearly at 100 μm on the lower 1.5 mm of the probe and a maximum width of 265 μm [Fig. 4(b)]. The custom designed printed circuit board connects the polymer probe to an Omnetics connector via a zero insertion force connector for mechanical and electrical coupling [Fig. 4(c)]. As shown in Figure 4(d,e), after the electrochemical deposition of PEDOT:PSS, the magnitude of the EIS was reduced and the phase became more positive suggesting a larger effective surface area due to the presence of the conductive polymer on the microelectrode surface and indicative of the electrode being capable of electrochemical charge transfer. Such changes in the impedance profile after electrochemical deposition of PEDOT:PSS are consistent with prior work.[24,25] The magnitude of the impedance at 1 kHz was decreased from 880.1 ± 51.8 kΩ to 51.3 ± 4.1 kΩ, whereas the phase was changed from −70.4 ± 2.7° to −40.3 ± 1.3° after the deposition (N = 32 microelectrodes).

In vivo recordings and impedance

As proof of concept, two animals were implanted with the SMP intracortical probes consisting of a polymer formulations with 47 mol % TCMDA. Recordings were taken of spontaneous neural activity from awake and moving rats revealing well distinguished single units with a signal-to-noise ratio of 5–10 over the duration of the 11 week study (Fig. 5). With the exception of a transient reduction in activity after the first week of implantation,

stable recordings were observed throughout the study [Fig. 6(a)]. In addition, the SMP intracortical probes showed a stable impedance magnitude [Fig. 6(b)] and phase [Fig. 6(c)] at 1 kHz that, after the second week of implantation, remained consistent throughout the study suggesting device stability *in vivo*.

Device capture immunohistochemistry

To visualize the tissue response to the implanted intracortical probe, device capture IHC was used. In Figure 7(a), a confocal image of a sagittal slice containing an intracortical probe is shown with stained tissue using DAPI, a fluorescent probe labeling cell nuclei (blue), labeled antibodies against NeuN for neuronal nuclei (yellow), and GFAP for activated astrocytes (green). Figure 7(b) shows NeuN and GFAP fluorescence intensity averaged along the length of the intracortical probe as function of distance perpendicular to the probe edge. The intensity values reaches 80% of the baseline levels within 50 μm from the insertion site. The degree of neuronal loss and astrocyte activation as shown by NeuN and GFAP labeling, respectively, is comparable to that previously reported for implantable probes.[6,26] In summary, these proof-of-concept experiments demonstrate that functional SMP-based intracortical probes can be successfully fabricated where multichannel recordings can be performed to isolate single units for >2 months.

DISCUSSION

Based on prior work, it is widely acknowledged in the neural interfaces field that the mismatch between the mechanical properties of the biological substrate and conventional implantable devices poses a barrier in demonstrating long term viability of neural recording probes. This work demonstrated that a multichannel intracortical probe can be fabricated using SMPs, that the mechanical behavior of the substrate is stable when glassy for surgical insertion, and again stable after softening for long term use. In addition, the softening is predictable and the overall device is capable of recording neural single units from the rat motor cortex for 77 days.

There has been significant prior work exploring the development of microelectrodes that provide enhanced flexibility over conventional silicon based substrates. Materials including polyimide,[27] SU-8,[28] poly(vinyl alcohol)/poly(acrylic acid) hydrogel,[29] and parylene[30,31] have been exploited. While reduced, the modulus of these polymeric materials and brain tissue still differ by at least five orders of magnitude. More recently, Capadona's group demonstrated a bioinspired, mechanically dynamic nanocomposite material for intracortical probes.[10,32] Implanted nanocomposite-based microelectrodes exhibit a modulus that rapidly transitions from 5 GPa to 12 Mpa[32] and result in negligible neuron loss at the device-tissue interface after 4 months in the brain.[33] For these bioinspired devices, however, softening occurs with a 70% increase in volume due to water absorption. Such a volume change potentially poses limitations on long term device fidelity by disrupting the surrounding tissue and compromising electrical connectivity to external devices. A key advantage of the SMP-based devices is that the degree of softening can be tuned with subtle changes in chemistry where the mechanical transition is accompanied by a relatively minor change in the volume of ~2–3%.

Figure 1 presents preliminary evidence of the ability to modify the underlying substrate structure in a way compatible with all of the processing necessary to build functional neural recording probes, such that the final mechanical properties (specifically modulus mismatch with surrounding tissue) can be tuned. These design techniques to build custom modulus implantable bioelectronics that may more readily interface with different regions in the body beyond shallow cortical regions. This design space would not be possible without polymer systems that exhibit swelling that does not damage the embedded thin film electronics, as described in Figure 2, and also is compatible with the electrode materials shown in Figure 4. While many different electrode materials are envisioned for manipulating the change injection capacity at the biotic–abiotic interface, including sputtered iridium oxide films, titanium nitride films, and platinum in various manifestations, PEDOT:PSS provides an excellent, well-studied polymer-based electrode that can be added through an straightforward electro-deposition process. Other materials (sputtered or e-beam evaporated) may require many additional photomasks and photolithographic steps which add to the complexity of the device and the chances for inconsistencies during the development process. A goal of this work was to provide preliminary support that from start to finish, a neural device could be designed and manufactured with new chemistries, materials, and techniques that could provide a stable recording platform for cortical neural activity. Most significantly, Figure 5 demonstrates the ability of these custom made devices to resolve single units both at day 2 after implant and after 77 days in the body. To our knowledge this is first example of long-term, stable single unit recordings of photolithography-compatible softening bioelectronics, even despite the fact that there is an increase in the activated astrocytes and a reduction in neurons within 100 mm of the implanted shank (Fig. 7). Future work will look to ways to reduce probe dimensions, alter surface chemistry, change electrode size and spacing and find different ways to tether or wireless connect softening neural probes. However, this article presents a minimum functional device, despite the noted limitations, that can serve as a benchmark for improvement of future softening bioelectronics. We present a tool set that will allow future researchers to more deeply study the effects of micromotion and other phenomena of implanted devices of different moduli on tissue. In the future, we anticipate that researchers will vary shank dimensions and utilize more complex composites built around these and other softening systems to target deeper brain regions with softening, penetrating neural probes. Interesting areas of future study will also include new ways to bond and connect to softening probes such that information can be more readily transmitted. These will include smaller connectors and wires or wireless antennae for power transfer and information exchange.

CONCLUSION

We have demonstrated the first low-swelling, softening substrate compatible with standard photolithography processes that is capable of stable single-unit cortical recordings for >2 months. We show a process whereby electrode geometries approach the size scale of neural cell bodies such that devices can achieve local specificity in recording. We demonstrate materials that soften in both accelerated aging tests, *in vitro* tests and *in vivo* toward the modulus of brain tissue, from ~600 MPa in shear modulus, sufficient for surgical insertion several millimeters into the cortex. With this platform technology, future work will

systematically explore the role of softening for intracortical probe histological and recording performance. In addition, the SMP devices can be processed using approaches suitable for manufacturing, which increases the reproducibility of the fabricated probes and enables a process for eventual technology translation and dissemination.

Contract grant sponsor:

Texas Biomedical Devices Center, the Defense Advanced Research Projects Agency Young Faculty Award Program (WEV) and DARPA MTO (JJP) under the auspices of Dr. Jack Judy through the Space and Naval Warfare Systems Center, Pacific; contract grant number: N66001-12-1-4026 (to J.J.P.)

REFERENCES

1. Kipke DR, Shain W, Buzsáki G, Fetz E, Henderson JM, Hetke, Schalk G. Advanced neurotechnologies for chronic neural interfaces: New horizons and clinical opportunities. J Neurosci 2008;28: 11830–11838. [PubMed: 19005048]
2. Grill WM, Norman SE, Bellamkonda RV. Implanted neural interfaces: Biochallenges and engineered solutions. Annu Rev Biomed Eng 2009;11:1–24. [PubMed: 19400710]
3. Homer ML, Nurmikko AV, Donoghue JP, Hochberg LR. Implants and decoding for intracortical brain computer interfaces. Annu Rev Biomed Eng 2013;15:383–405. [PubMed: 23862678]
4. Bensmaia SJ, Miller LE. Restoring sensorimotor function through intracortical interfaces: Progress and looming challenges. Nat Rev Neurosci 2014;15:313–325. [PubMed: 24739786]
5. Barrese JC, Rao N, Paroo K, Triebwasser C, Vargas-Irwin C, Franquemont L, Donoghue JP. Failure mode analysis of silicon-based intracortical microelectrode arrays in non-human primates. J Neural Eng 2013;10:066014. [PubMed: 24216311]
6. Barrese JC, Aceros J, Donoghue JP. Scanning electron microscopy of chronically implanted intracortical microelectrode arrays in non-human primates. J Neural Eng 2016;13:026003. [PubMed: 26824680]
7. Biran R, Martin DC, Tresco PA. Neuronal cell loss accompanies the brain tissue response to chronically implanted silicon microelectrode arrays. Exp Neurol 2005;195:115–126. [PubMed: 16045910]
8. Polikov VS, Tresco PA, Reichert WM. Response of brain tissue to chronically implanted neural electrodes. J Neurosci Methods 2005;148:1–18. [PubMed: 16198003]
9. Harris JP, Capadona JR, Miller RH, Healy BC, Shanmuganathan K, Rowan SJ, Weder C, Tyler DJ. Mechanically adaptive intracortical implants improve the proximity of neuronal cell bodies. J Neural Eng 2011;8:066011. [PubMed: 22049097]
10. Hess AE, Capadona JR, Shanmuganathan K, Hsu L, Rowan SJ, Weder C, Tyler D, Zorman C. Development of a stimuli-responsive polymer nanocomposite toward biologically optimized, MEMS-based neural probes. J Micromech Microeng 2011; 21:054009.
11. Kim DH, Abidian M, Martin DC. Conducting polymers grown in hydrogel scaffolds coated on neural prosthetic devices. J Biomed Mater Res A 2004;71:577–585. [PubMed: 15514937]
12. Ware T, Simon D, Arreaga-Salas DE, Reeder J, Rennaker R, Keefer EW, Voit W. Fabrication of responsive, softening neural interfaces. Adv Funct Mater 2012;22:3470–3479.
13. Subbaroyan J, Martin DC, Kipke DR. A finite-element model of the mechanical effects of implantable microelectrodes in the cerebral cortex. J Neural Eng 2005;2:103–113. [PubMed: 16317234]
14. Mahi H, Rodrigue D. Linear and non-linear viscoelastic properties of ethylene vinyl acetate/nano-crystalline cellulose composites. Rheol Acta 2012;51:127–142.
15. Ware T, Simon D, Liu C, Musa T, Vasudevan S, Sloan AM, Keefer EW, Rennaker RL, Voit W. Thiol-ene/Acrylate substrates for softening intracortical electrodes. J Biomed Mater Res B Appl Biomater 2014;102:1–11. [PubMed: 23666562]
16. Hukins D, Mahomed A, Kukureka S. Accelerated aging for testing polymeric biomaterials and medical devices. Med Eng Phys 2008; 30:1270–1274. [PubMed: 18692425]

17. Cui X, Martin DC. Electrochemical deposition and characterization of poly(3,4-ethylenedioxythiophene) on neural microelectrode arrays. Sensor Actuat B Chem 2003;89:92–102.
18. Charkhkar H, Frewin C, Nezafati M, Knaack GL, Peixoto N, Saddow SE, Pancrazio JJ. Use of cortical neuronal networks for *in vitro* material biocompatibility testing. Biosens Bioelectron 2014;53:316–323. [PubMed: 24176966]
19. Ward MP, Rajdev P, Ellison C, Irazoqui PP. Toward a comparison of microelectrodes for acute and chronic recordings. Brain Res 2009;1282:183–200. [PubMed: 19486899]
20. Knaack GL, Charkhkar H, Hamilton FW, Peixoto N, O'Shaughnessy TJ, Pancrazio JJ. Differential responses to ω-agatoxin IVA in murine frontal cortex and spinal cord derived neuronal networks. Neurotoxicology 2013;37:19–25. [PubMed: 23523780]
21. Ludwig KA, Miriani RM, Langhals NB, Joseph MD, Anderson DJ, Kipke DR. Using a common average reference to improve cortical neuron recordings from microelectrode arrays. J Neurophysiol 2009;101:1679–1688. [PubMed: 19109453]
22. Woolley AJ, Desai HA, Steckbeck MA, Patel NK, Otto KJ. In situ characterization of the brain–microdevice interface using device capture histology. J Neurosci Methods 2011;201:67–77. [PubMed: 21802446]
23. Harry GJ, Billingsley M, Bruinink A, Campbell IL, Classen W, Dorman DC, Galli C, Ray D, Smith RA, Tilson HA. In vitro techniques for the assessment of neurotoxicity. Environ Health Perspect 1998;106:131–158. [PubMed: 9539010]
24. Cogan SF. Neural stimulation and recording electrodes. Annu Rev Biomed Eng 2008;10:275–309. [PubMed: 18429704]
25. Mandal HS, Knaack GL, Charkhkar H, McHail DG, Kastee JS, Dumas TC, Peixoto N, Rubinson JF, Pancrazio JJ. Improving the performance of poly(3,4-ethylenedioxythiophene) for brain–machine interface applications. Acta Biomater 2014;10:2446–2454. [PubMed: 24576579]
26. Potter KA, Buck AC, Self WK, Callanan ME, Sunil S, Capadona JR. The effect of resveratrol on neurodegeneration and blood brain barrier stability surrounding intracortical microelectrodes. Biomaterials 2013;34:7001–7015. [PubMed: 23791503]
27. Rousche PJ, Pellinen, Pivin DP Jr, Williams JC, Vetter RJ, Kipke DR. Flexible polyimide-based intracortical electrode arrays with bioactive capability. IEEE Trans Biomed Eng 2001;48:361–371. [PubMed: 11327505]
28. Fernández LJ, Altuna A, Tijero M, Gabriel G, Villa R, Rodríguez MJ, Batlle M, Vilares R, Berganzo J, Blanco F. Study of functional viability of SU-8-based microneedles for neural applications. J Micromech Microeng 2009;19:025007.
29. Lu Y, Wang D, Li T, Zhao X, Cao Y, Yang H, Duan YY. Poly (vinyl alcohol)/poly (acrylic acid) hydrogel coatings for improving electrode–neural tissue interface. Biomaterials 2009;30:4143–4151. [PubMed: 19467702]
30. Takeuchi S, Ziegler D, Yoshida Y, Mabuchi K, Suzuki T. Parylene flexible neural probes integrated with microfluidic channels. Lab Chip 2005;5:519–523. [PubMed: 15856088]
31. Wester B, Lee R, LaPlaca M. Development and characterization of *in vivo* flexible electrodes compatible with large tissue displacements. J Neural Eng 2009;6:024002. [PubMed: 19255461]
32. Harris JP, Hess AE, Rowan SJ, Weder C, Zorman CA, Tyler DJ, Capadona JR. *In vivo* deployment of mechanically adaptive nano-composites for intracortical microelectrodes. J Neural Eng 2011;8:046010. [PubMed: 21654037]
33. Nguyen JK, Park DJ, Skousen JL, Hess-Dunning AE, Tyler DJ, Rowan SJ, Weder C, Capadona JR. Mechanically-compliant intracortical implants reduce the neuroinflammatory response. J Neural Eng 2014;11:056014. [PubMed: 25125443]

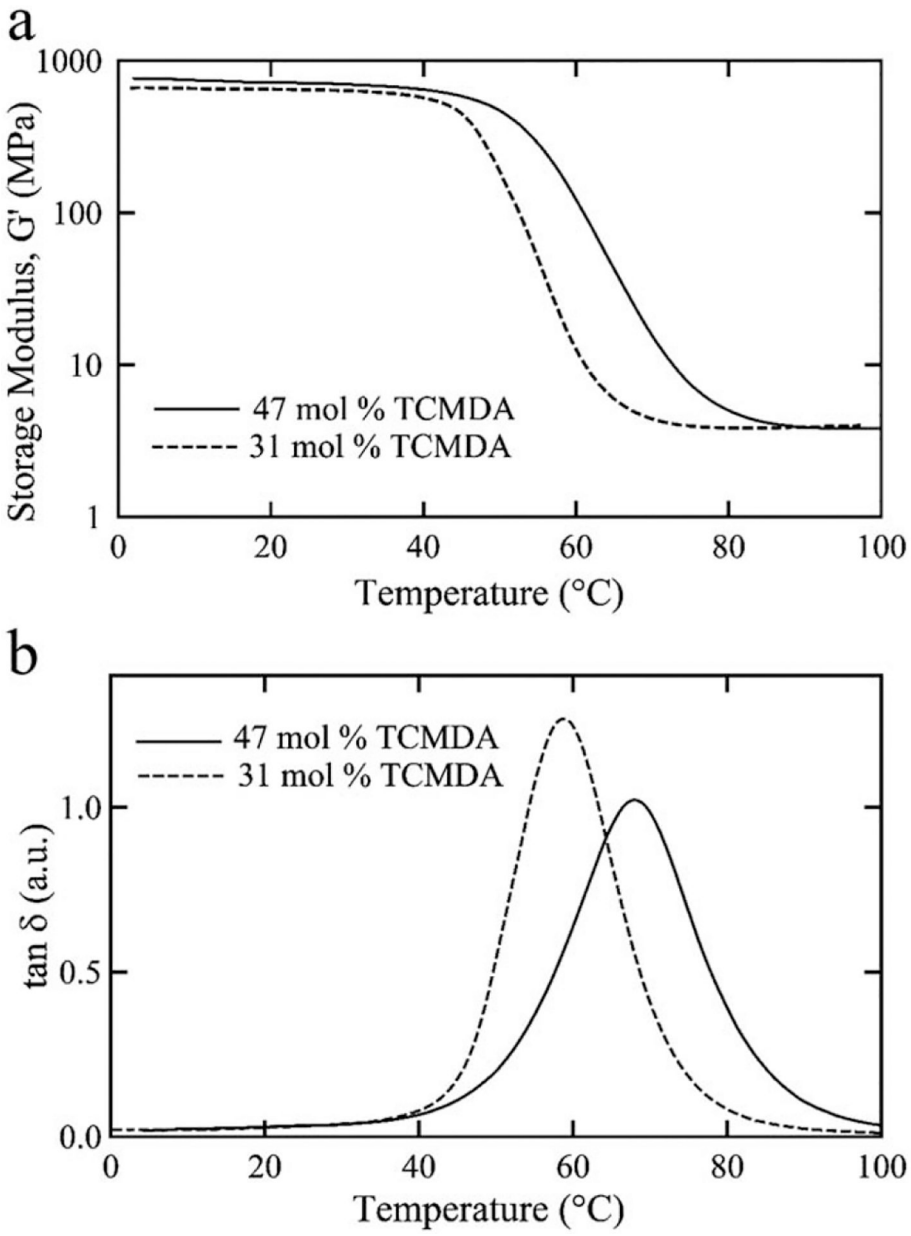

FIGURE 1.

Thermomechanical characterization of the thiol-ene/acrylate polymer compositions. Comparison for 31 and 47% TCMDA of the storage modulus (a) and tan d (b) as a function of temperature.

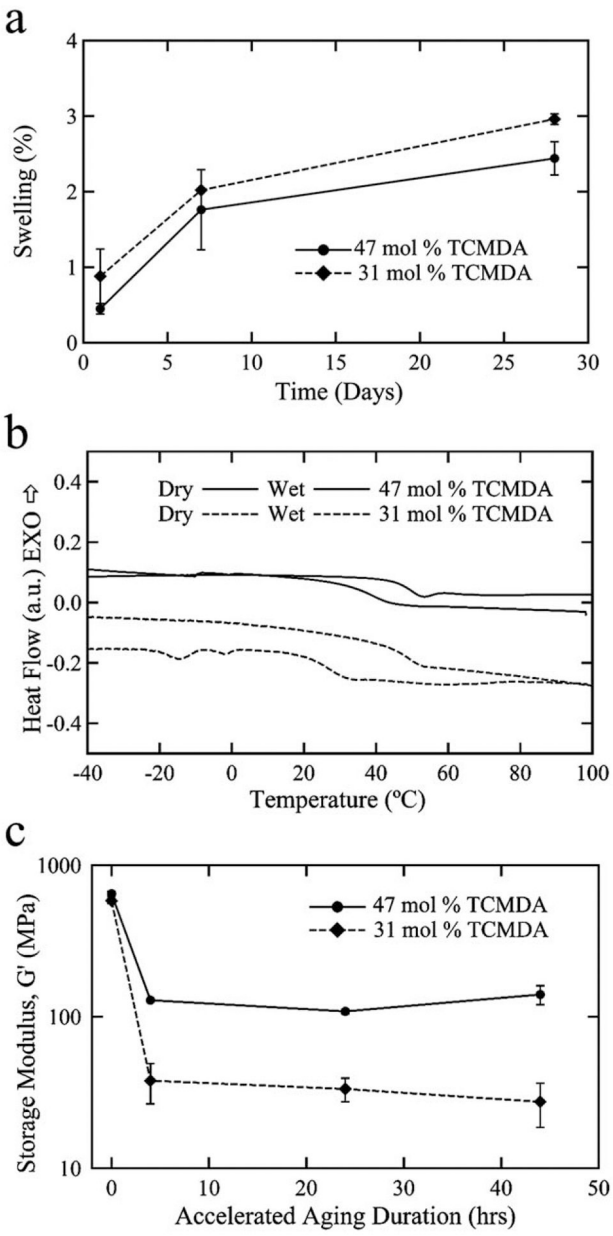

FIGURE 2.

Thermomechanical properties of the thiol-ene/acrylate polymer samples *in vitro*. Plots demonstrating low degree of moisture absorption of each polymer composition in phosphate-buffered saline at 37°C (a). The leftward shift in T_g for the polymer formulation from dry and to conditions (b). Characterization of the storage modulus, determined at 37°C, under accelerated aging conditions for the two polymer compositions indicating a projected softening for at least 77 days *in vivo* (c).

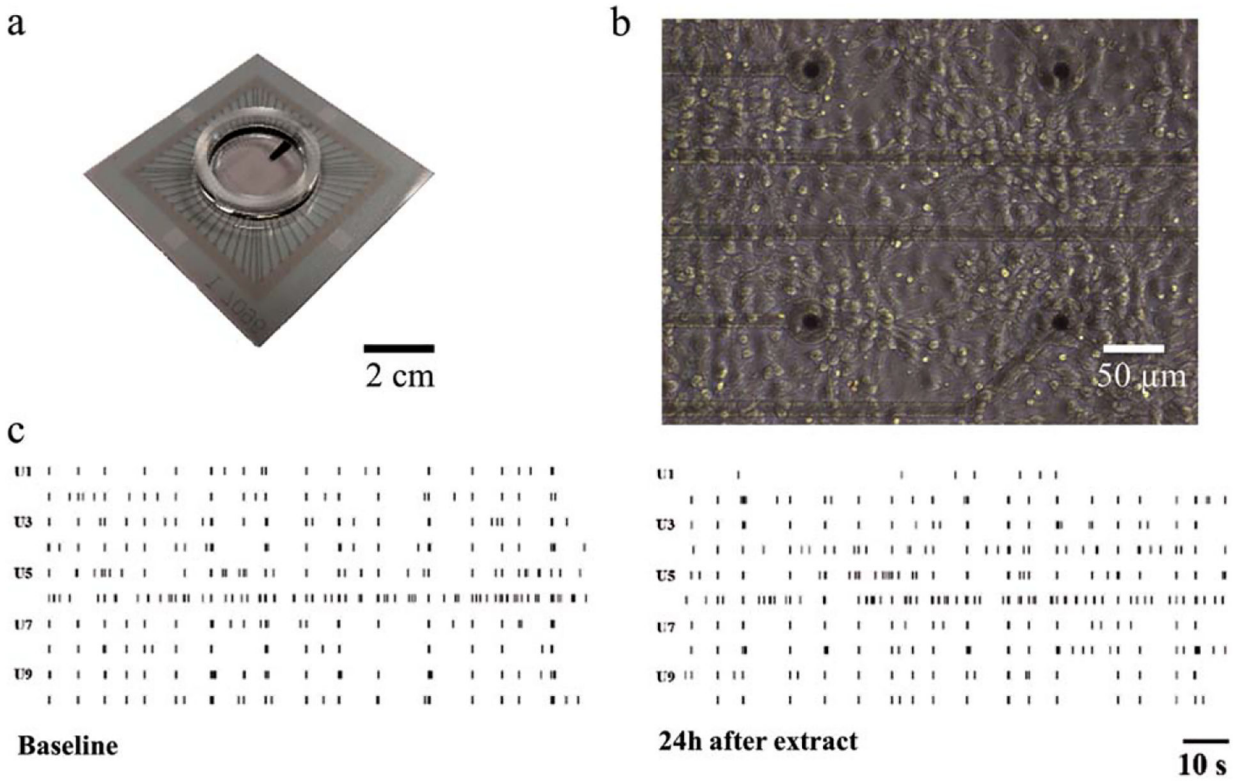

FIGURE 3.

In vitro functional neurotoxicity testing of the SMP materials. Using commercially available microelectrode array dishes (a), primary cortical neurons from embryonic mice were seeded on MEA substrates and were cultured for at least 21 days *in vitro* to produce stable and mature networks (b). Raster plots of spontaneous single unit spike activity from a representative cultured neuronal network before (c, left) and 24 h post exposure (c, right) of extracts from thiol-ene/acrylate polymer substrates showing little or no response to the softening materials.

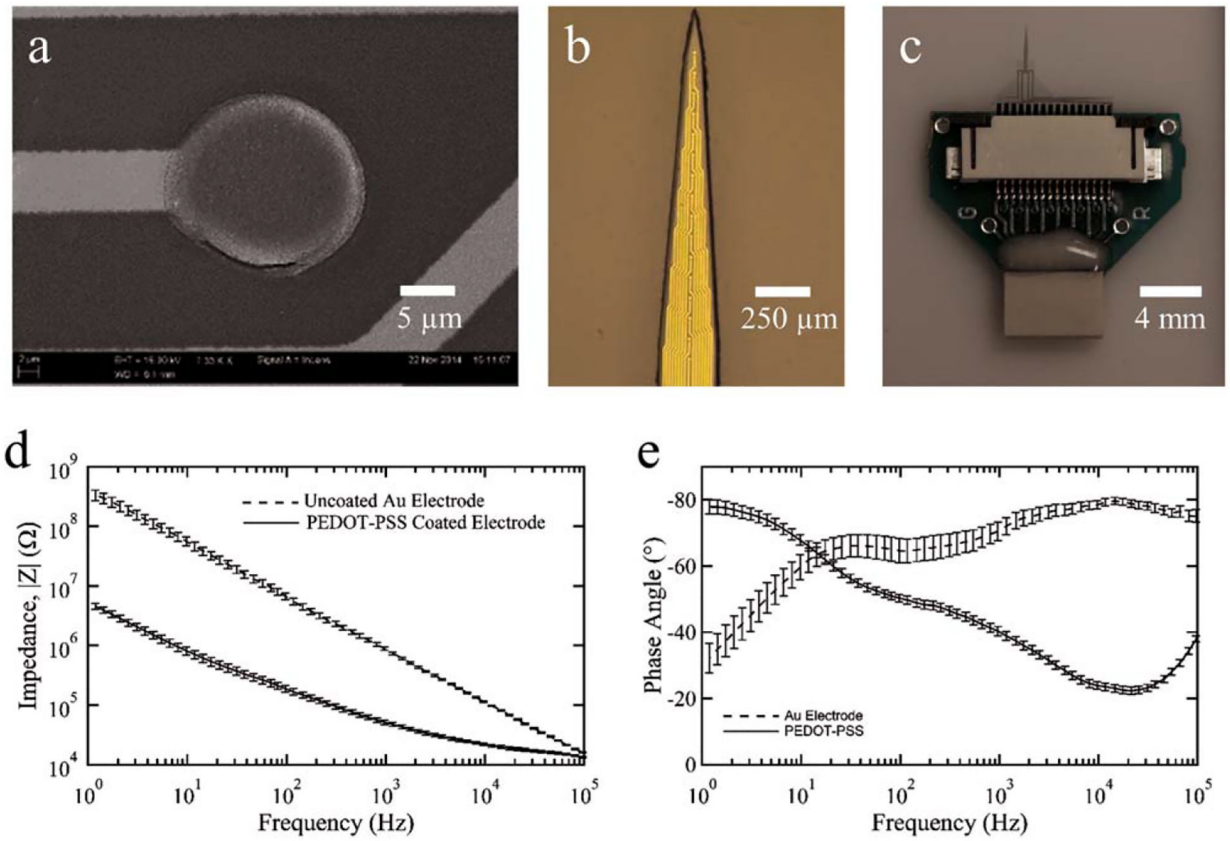

FIGURE 4.

Fabrication and packaging of the novel SMP-based intracortical probe using 47 mol % TCMDA. Scanning electron microscopy image of the thin film layers of Au and parylene-C created using photolithography to produce traces and recording sites (a). To reduce the impedance of each microelectrode, a layer of PEDOT:PSS was deposited on each site. Photomicrograph of the penetrating portion of the approximately 2.5 mm long intracortical probe showing several of the 16 evenly spaced microelectrode sites along the lower 1.5 mm region of the device (b). Image showing the custom circuit board designed and fabricated to interface the SMP probe with the head stage of recording system (c). Electrochemical impedance spectroscopy of thiol-ene/acrylate probes before (Au only) and after PEDOT:PSS electroplating showing impedance magnitude (d) and phase (e) as a function of frequency. Data are shown as mean ± standard error of the mean (n = 32 microelectrodes).

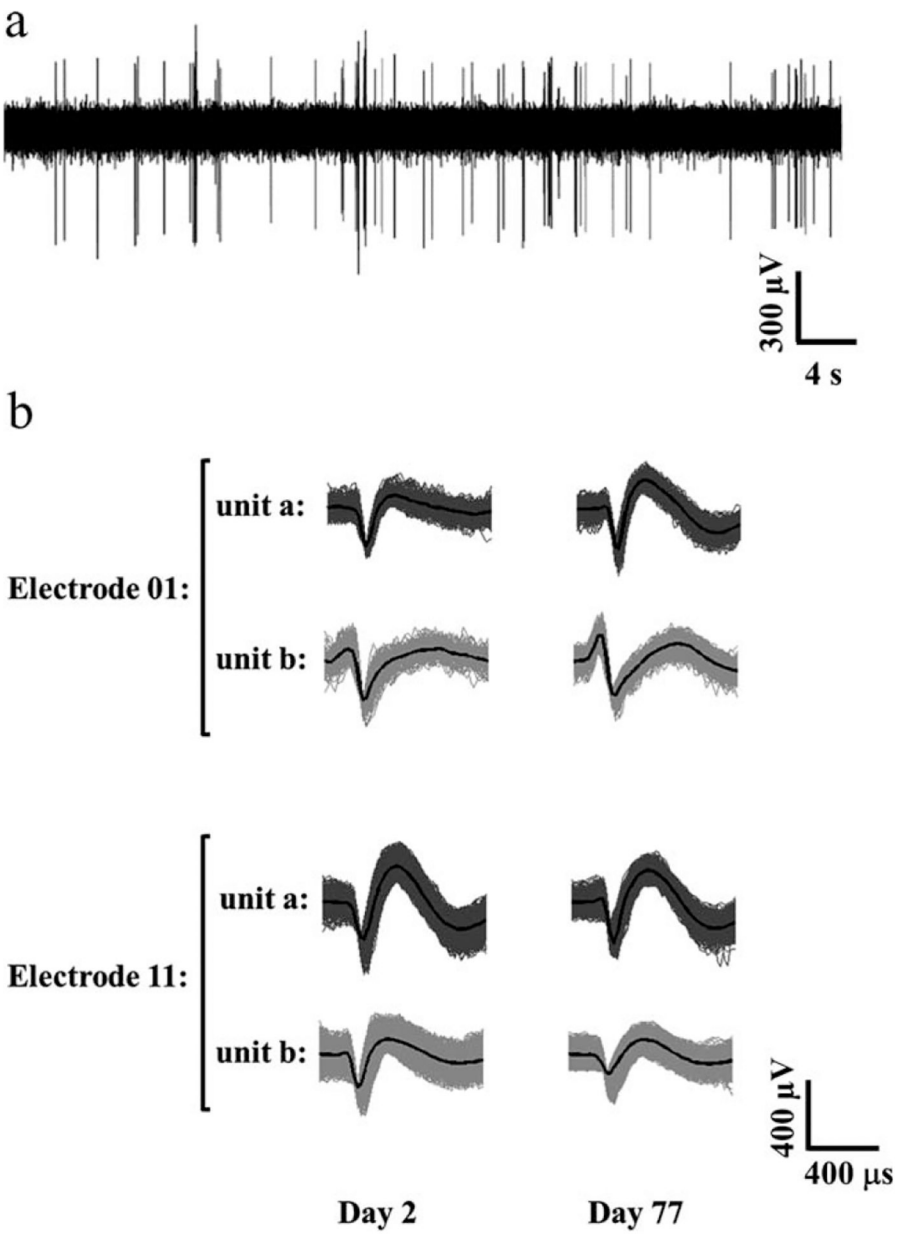

FIGURE 5.

Single unit recording from the SMP-based intracortical probe. Recording from a typical microelectrode recording site from day 2 *in vivo*. The signal-to-noise ratio for the recordings ranged from 5–10 (a). Examples of well-resolved and distinguished single units from the same SMP-based intracortical probe detected on day 2 and day 77 of the implantation (b).

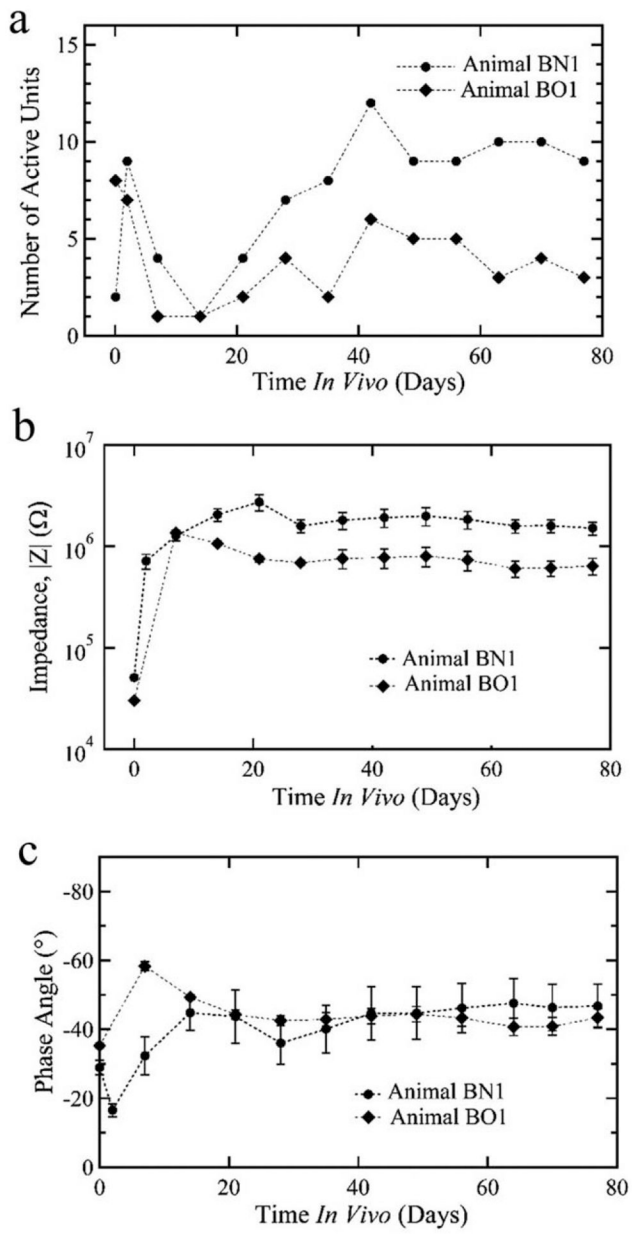

FIGURE 6.

Novel intracortical probe performance *in vivo* over 11 weeks of implantation. With the exception of a brief period within the first 2 weeks of implantation, both of the animals demonstrated active single units over the duration of the study (a). Likewise, the impedance magnitude (b) and phase (c) across the microelectrode sites was consistent during implantation indicating stability of the SMP intracortical probe.

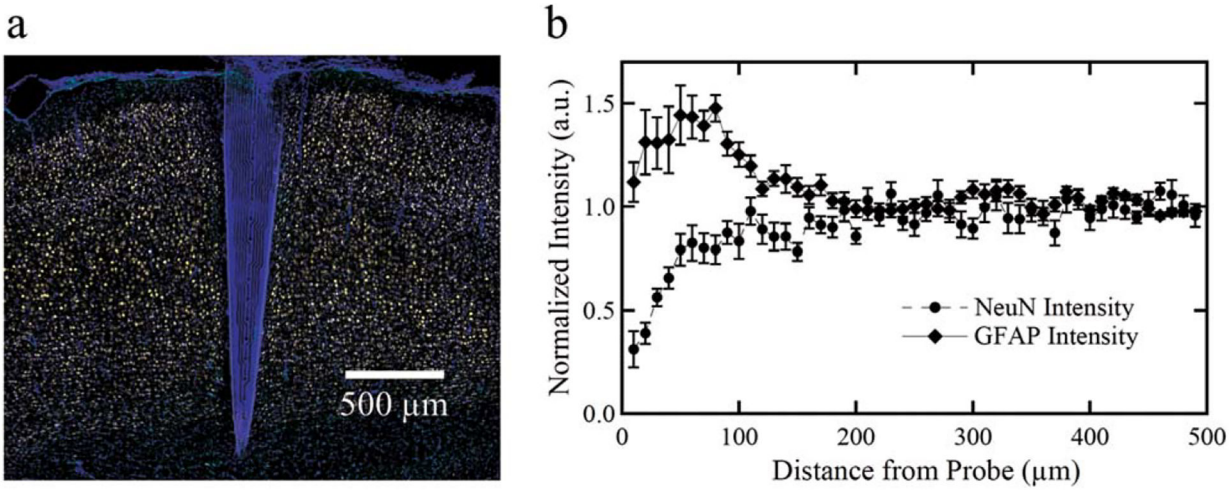

FIGURE 7.

Device capture immunohistochemical analysis of implanted SMP cortical probe. The Confocal optical micrograph of an SMP intracortical probe in brain tissue for 77 days where the colors represent NeuN (yellow), GFAP (green), and DAPI (blue). The device was autofluorescent under the UV emission. Normalized intensity profile for NeuN and GFAP as a function of distance from the probe (b) indicates that there is a reduction of neurons and elevation of activated astrocytes proximal to the probe insertion site.